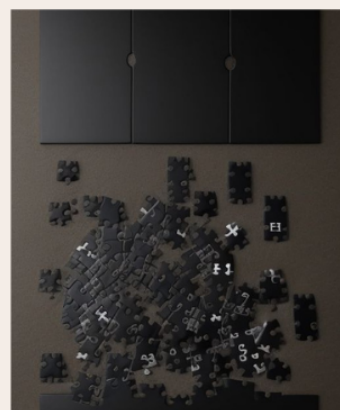


SCIENCE ASCEND

14-21 October 2024



What is in?

Astrophysics: Three separate studies on Gliese 229B, protoplanetary disk studies and more

Analytical Chem.: Mass spectrometry use, sensitive NMR, fluorescence and electrochemistry

Remote Sensing: Better disaster aftermath estimation, new SAM models, and a comprehensive review on visual language models

Environmental Chem.: Organic peroxide identification, air pollution deweathering, and dissolved organic matter surrogate

Data Decomposition: Missing entry completion, root cause search and more

ISSN:3062-0090

FIRE Arařtırma Eđitim Ltd. řti. Vol:1 Issue:7



Science Ascend

Rising to New Heights of Discovery!

Science Ascend teleports you to the frontiers of science. It compiles and discuss the scientific research preprints from arXiv and chemRxiv just from the previous week to be cognizant of the *state-of-the-art* of knowledge in astrophysics, analytical chemistry, environmental chemistry, remote sensing, and applied statistics/data science. Light from the *Science Ascend* will keep brightening the dark horizon beyond the limits of our comprehension. FIRE Araştırma Eğitim Ltd. Şti. guarantees the weekly publication and dissemination of this journal, and make it available for everyone at most fifteen days after its publication freely.

Publisher: FIRE Araştırma Eğitim Ltd. Şti.
Media: Online Journal
Responsible person: Yasin Güray Hatipoğlu
Editor-in-chief: Yasin Güray Hatipoğlu
Editor: Yasin Güray Hatipoğlu
Frequency: Once a week
Address: Yıldızevler Mah. Kişinev Cad. No:10
Çankaya/Ankara/Türkiye
Website: <https://fire-ae.github.io>

This issue: October 21, 2024

Volume: 1

Issue Number: 7

All rights reserved.



Bilim Yükselişi

Keşfin Yeni Yükseklerine Ulaşmak!

Science Ascend sizi bilimin sınırlarına ışınlar. Astrofizik, analitik kimya, çevre kimyası, uzaktan algılama ve uygulamalı istatistik/veri bilimi alanlarındaki bilgi birikiminin *en son durumu* hakkında bilgi sahibi olmak için arXiv ve chemRxiv'den sadece bir önceki haftaya ait bilimsel araştırma ön baskılarını derler ve tartışır. *Bilim Yükselişi*'nden gelen ışık, kavrayışımızın sınırlarının ötesindeki karanlık ufku aydınlatmaya devam edecektir. FIRE Araştırma Eğitim Ltd. Şti. bu derginin haftalık olarak yayımlanmasını, dağıtılmasını ve yayımlandıktan en geç on beş gün sonra ücretsiz olarak herkesin erişimine açılmasını garanti eder.

Yayıncı: FIRE Araştırma Eğitim Ltd. Şti.
Ortam: Online Journal
Sorumlu Kişi: Yasin Güray Hatipoğlu
Yazı İşleri Müdürü: Yasin Güray Hatipoğlu
Editör: Yasin Güray Hatipoğlu
Yayımlanma Sıklığı: Haftada bir kez
Adres: Yıldızevler Mah. Kişinev Cad. No:10
Çankaya/Ankara/Türkiye
Website: <https://fire-ae.github.io>

Bu sayı: 21 Ekim 2024

Cilt: 1

Sayı Numarası: 7

Tüm hakları saklıdır.

Contents

Last week in Astrophysics	4
Astrochemistry	4
Stellar Systems - Populations - Clusters	4
Single Star System (Star, Exoplanet) . .	4
Exoplanet Atmospheres	5
Protoplanetary - Circumstellar Disks	6
Sun	7
Mars	7
0.1 Jupiter	7
Jupiter	7
0.2 Solar System Ice Giants	7
Solar System Ice Giants	7
Near-Earth Objects - Asteroids - Comets	7
Moon	8
Earth - Space relationship	8
Magnetohydrodynamics	8
Last week in Analytical Chemistry	9
Mass Spectroscopy	9
Immunoassays	9
Electrochemistry	10
Nuclear Magnetic Resonance - NMR . .	10
Fluorescence	10
Last week in Remote Sensing	11
Segmentation	11
Modelling-Forecast	11
Object Detection	11
Last week in Environmental Chemistry	12
Last week in Data Decomposition/Transformation	13
Denoising	13
Modelling	13
Missing Data Imputation	13

Foreword

Greetings everyone!

This issue covers the preprints between October 14-21, 2024.

Astrophysics had many studies on the Solar System, protoplanetary disks, and more interestingly, three separate research groups published a preprint on Gliese 229B, where all estimated that it is actually a brown dwarf duo with similar masses.

One multifaceted workflow in the remote sensing preprints had the Adaptive Disaster Interpretation where it can be highly beneficial to researchers and policy makers alike.

Analytical and Environmental Chemistry preprints were comparatively low in number but not in quality.

For the data decomposition methods, interesting studies took place for missing entry imputations, root cause identification, denoising, and other tasks.

See you next week!

Güray Hatipoğlu

Last week in Astrophysics

Author: *Yasin Güray Hatipoğlu*

The preprints summarized here were published between October 15 - October 21, 2024. These are from arXiv's astro.EP cross-fields

Astrochemistry

Tokadjian et al.[1] forward modeled of Archean and Proterozoic (4 to 2.5 gigayears before and 2.5 to 0.5 gigayears before, respectively) Earth atmosphere with the ExoRel code to check the detectability of methane, carbon dioxide, carbon monoxide, and nitrous oxide from the reflected light spectrum ranging 0.25 to 1.8 μm . They applied a Gaussian photon noise to the retrieved spectra for an SNR of 20 at 0.75 μm with resolutions 7, 140, and 70 for UV, optical, and near IR ranges of this wavelength range. They specifically stated that the ratio of methane to carbon dioxide (CH_4/CO_2) and N_2O individually might be better targets to detect.

Stellar Systems - Populations - Clusters

Yamaguchi and El-Badry[2] considered the case that *Kepler* data had revealed five self-lensing binaries (SLB), while no SLB was found with the TESS data, even considering the fact that TESS monitors the same period of the sky uninterrupted for 25 days for the most stars. They started with approximately 2 million light curves around 900 000 unique sources, filtering the sample according to the root mean square error in flux smaller than 0.001 which would correspond to a self-lensing pulse from a WD companion. Then, they tried to find the peak more reminiscent of the self-lensing with a Gaussian Process fitting using the Bayesian Information Criterion via the george Python package. They put additional criteria to down the sample around 800, then selected a further 72 “Gold” samples as the most promising, and reported that in total, TESS observed around 4 times more detectable SLBs than *Kepler*.

O'Connor and Lai[3] studied the origin of the metal pollution in Sun-like stars from the perspective of engulfing ultra-short-period (USP) planets. The calculations used a low-eccentricity migration scenario in mind, in which the future USP planet's eccentricity remained low because of the interplanetary interactions. Among many interesting insights, they reported that most FGK-type dwarfs should have a compact multi-planetary

system with the innermost having 5 times Earth mass and smaller than 0.1 au semi-major axis.

Ofir et al.[4] examined the 64 systems containing 218 planets with PyDynamicalLC, and among them, 88 gained a higher than 3σ significant masses, with 23 had their first mass determination. The data was from the *Kepler* mission and the technique was the Transit Timing Variation. The PyDynamicalLC package utilizes TTVFaster and MultiNest packages' techniques and develops over them. Their approach was particularly effective for the comparatively low-quality, low SNR TTV signals.

Lin et al.[5] examined the hypothesis of the “naked core” hypothesis, where an unlikely high-density exoplanet was assumed to be a remnant core of previous giant planets with a lost envelope. First, they constructed a planetary interior model with a nonrotation and spherically symmetric planet in hydrostatic equilibrium. The outer boundary conditions for the naked-core planets were their equilibrium pressure, while for self-compressed ones it was a set 0.1 bar. Their planets had a fully differentiated Fe (iron) core, MgSiO_3 mantle, and H/He or H_2O primordial envelope (it is mostly similar to an atmosphere, but it still considers parts from the top to the mantle) to account gas and ice giants, respectively. AQUA was chosen to model H_2O envelope, while for H/He a 0.275 Helium fraction and a wide Pressure-Temperature range EOS database were adopted. The magma ocean profile was considered with an adiabatic temperature profile, and then, they evolved the naked core. They generally found the naked-core hypothesis unlikely, especially with the added detail of estimated fuzzy cores of Jupiter and Saturn.

Single Star System (Star, Exoplanet)

Staelen et al.[6] examined the oblate, spheroid, and prolate-shaped internal cores of celestial bodies. Their approach included a composite of two homogeneous layers with different characteristics and rotations. They started from the slow rotators and also discussed the potential extension to the fast rotators in case of the following core-envelope matches: oblate-oblate (OO), oblate-prolate (OP), PO, and PP. They ruled out the prolate envelope cases as they can not be at equilibrium, but a prolate core can be permitted along with OO cases.

Pucacco[7] studied the dynamical stability of the *de Sitter* equilibria for the multiresonant planetary systems. Pucacco applied the theoretical underpinnings presented in the first parts of the paper to the Jupiter-Galilean system (Io, Europa, and Ganymede) and the Gliese 876 system. It was

reported that the sequence of Laplace-resonant equilibrium configurations could be parametrised with the single resonance proximity parameter, and although only first-order resonant terms can give explicit solutions for this sequence and the bifurcation threshold, numerical root-finding methods were necessary for more accurate estimations.

Yu et al.[8] attempted to model the stellar activity-related signals with a physics-driven Gaussian process (multi-GP) framework from the time series of spectral line profiles or cross-correlation functions, simulated it, made injected-retrieval tests, and also worked with the HARPS-N solar data and HARPS observations of HD 13808. Firstly, they explained the FF' framework (F is flux in specific times), how the line-of-sight velocity changes similar to the derivative of F (which is F') and up-flow velocity behaves as F. The multi-GP framework involves a quasi-periodic GP modeling of F^2 , and consequently, G' is proportional to the FF'. Rather than modeling the line profile, they subtracted the baseline devoid of active regions from the line profiles and worked on the perturbations. They divided the effects on the stellar line profile active regions into two: the photometric effect, in which a dark spot or bright faculae may change the mean stellar line profile in a given point of a star, and the inhibition of convective blueshift effect, which, in a simplified manner, the magnetic field of the active regions result in a local redshift. After constructing the full model with two effects and combining the flux and flux derivative-related G and G', they approached the multi-GP framework without much inaccuracies regarding the higher-order effects. They implemented this with the S+LEAF 2 with Matérn 3/2 exponential periodic kernel to solve GP, and the joint posterior over the parameters was sampled with the PolyChord. The simulated data was generated with the Spot Oscillation and Planet Code (SOAP2). Their framework was robust in signal-to-noise ratios down to 100, and they found the approach successful overall.

Wang et al.[9] studied the PARSEC, BaSTI, MIST, and BY-SETTL models for ultraviolet emission fractionation for the F, G, K, and stars with the Galaxy Evolution Explorer far-UV and near-UV, China Space Station Telescope near-U, stellar effective temperatures, and Gaia BP-RP color differences. They plotted the magnitudes from the model estimations for different spectral types and compared them to the observations and reported the fractional UV contributions to the total stellar flux.

Venner et al.[10] reanalyzed HD 28185 from the 22 years of *Hipparcos-Gaia* radial velocity observations and precision astrometry measurements. They confirmed the HD 28185 temperate

giant planet character and presented new evidence for reclassifying HD 28185 c as a super-Jovian planet with around 25 years orbital period and 6 times Jupiter mass rather than a brown dwarf.

Whitebook et al.[11] discovered that the Gliese 229B system was a binary, with the other component being at least 15 times the Jupiter mass. They used Keck/NIRSPEC to obtain the spectra of the system in the R - 25000 high-resolution mode. The observations took place in March 2022 and November 2022, with the former in natural seeing mode with the 0.432" slit while the latter was in natural guide star adaptive optics with the 0.041" slit. They used a custom pipeline to reduce the data and after the radial velocity anomaly estimation, constrained the characteristics of the companion object. Similarly, Xuan et al.[12] studied the same system with the GRAVITY interferometer (data was reduced by ESO GRAVITY pipeline) and the CRRES+ spectrograph (reduced by *excalibuhr* of the Very Large Telescope (VLT) and came up with around 38 and 34.4 Jupiter masses for the two objects detected for the system. Moreover, they reported a semi-major axis value of 0.042 au for this tight brown dwarf binary system.¹

Marimbu and Lee[14] examined the erasure of the initial conditions in the multi-planetary systems, focusing on orbital periods. They used REBOUND N-body integrator with TRACE for up to 300 million years, 15 and 20 protoplanets separately with 500 randomized initializations in each. All planets had 2 times Earth mass. Through their simulations, they observed that till 100 million years the information regarding the initial conditions was erased.

Exoplanet Atmospheres

Agrawal and MacDonald[15] presented an open source molecular and atomic cross-section computation for exoplanetary atmospheres-Cthulhu, a Python package². It can automatically *summon* ExoMol and HITRAN/HITEMP lines to an HDF5 file and supports manual download of VALD line lists. It utilizes the Vectorised Voigt method and computes cross-sections after the location, temperature, pressure, and wavenumber range specifications.

Kawashima et al.[13] studied the Gl 229 B with the Subaru/IRD R approx. 70000 high-resolution spectroscopy. They retrieved a stellar-consistent C/O ratio, constrained the temperature and after considering the previously measured photometric magnitude, they stated that Gl

¹Also check another study under the Exoplanet Atmosphere category on Gl 229 B.[13]

²The related documentation can be found here.

229 B is a binary system.

Soni and Acharyya[16] constructed 1D chemical kinetic models to examine the impact of the vertical mixing in exoplanet atmospheres on the observed spectra from them. Their parameter space included the planet radius, reference pressure, eddy diffusion, surface gravity, internal and equilibrium temperature, and metallicity. Firstly, they explained the extreme atmospheric cases from very hot and very cold temperatures where the vertical mixing is not expected to play a significant role. They applied the vertical mixing time scale from the eddy diffusion and mixing length, the chemical time scale from the production and loss of a chemical species, and the quenching was incorporated with their newly-developed Python code and used the model in petitRADTRANS. They utilized the differences in vertical mixing under the same conditions for different chemicals to find the signature of vertical mixing in the transit spectra. In the end, they were more successful in putting constraints on eddy diffusion between 900 and 1400 K equilibrium temperatures.

Stangret et al.[17] studied the KELT-9b and KELT-20b (ultra-hot Jupiter exoplanets) atmospheres spectra considering Fe II winds with HRAPS-N spectrograph. They interpreted the blue-shifted signals found with the cross-correlation method KELT-9b as strong day-to-night side atmospheric winds, while for KELT-20b there was no conclusive evidence of such winds from Fe II signals.

Protoplanetary - Circumstellar Disks

Cesario et al.[18] and the LIFE Collaboration examined the potential design concepts for the Large Interferometer for Exoplanets (LIFE) to find transient magma oceans in cooling protoplanets with its space-based mid-infrared nulling interferometer. As it is not yet out, the work was done with the LIFE mission instrument simulator with optimistic, baseline, and pessimistic separate scenarios for the minimum and maximum wavelength and aperture diameter. Related code to reproduce the analysis is here. They estimated that within a 100-parsec distance, an Earth-sized magma ocean can be detected by the LIFE instrument in up to several hours of integration times at most. Moreover, they reported that shorter wavelength will be better at hot protoplanet detection, and the non-blackbody nature of the protoplanetary atmospheres, the inner working angle of the LIFE for distant systems, and a realistic instrumental noise model are needed to further mitigate the current limitations in estimations.

Dykes et al.[19] monitored the AB Aurigae protoplanetary disk with the Subaru Telescope's

SCEXAO/Coronagraphic High Angular Resolution Spectrograph (CHARIS) in 1.1-2.4 μm with an angular separation of 0.13" to 1.1" (on these they corresponded to the 20-175 astronomical units). They reduced the data with the standard CHARIS cube extraction pipeline, Data Processing Pipeline, and the pipeline's PDI module. They utilized the double difference method for removing the stellar point spread function (PSF). After the polarized light processing, they reported a wavelength-dependent shape change in the protoplanetary disk for different bands. They stated the successful higher-contrast result of the 22-channel polarized light contrary to the literature.

A different type of circumstellar disk was modelled by Fröhlich and Regály[20] as a disintegrating asteroid around a white dwarf star from its disintegration to the evolution of the remaining disintegrated parts. The main purpose was to examine the Calcium triplet (Ca II) emission around the metal-polluted white dwarfs. GFARGO2 modelled this below WD sublimation radius eccentric orbit asteroid. In the end, they stated that their simulation is in line with the observations of the persistent Ca II asymmetry, as the periodic reversal of blue-red shifts of this line could take place in the timescales of 10.6 to 177.4 days.

Zuleta et al.[21] examined a warped disk structure where inner and outer annuli have "tilt angles" between them. They estimated the molecular line emissions from their modelled warped disk with the RADMC3D code and they extended the eddy package to handle the cases of this study. They found out that their method is beneficial and robust in Atacama Large Millimeter/Submillimeter Array (ALMA) noises.

Ziampras et al.[22] modelled shadows in protoplanetary disks and investigated under what conditions the ring formation and/or substructures in the disk were favored. They used 2D PLUTO code, its FLD module and FARGO algorithm, and the HLLC Riemann solver. Then, to test if they can find these structures with the observations, RADMC-3D was used to generate synthetic observations. Their study had limitations for vertically integrated models rather than fully 3D ones, nevertheless, they were able to report that ALMA and VLT-SPHERE-like instruments could still detect the shadowing-related dynamics on the disk.

Xu et al.[23] simulated the gravitational instability by constructing 3D global models with the Athena++. They started with a gravitoturbulent disk and included three different ways to consider the cooling and radiation: a constant cooling coefficient, optically thin cooling, and optically thick cooling with full radiation transport. The results of the simulations were: the fragmentation into gravitationally bound parts was stochastic and

cooled and contracted clumps were better suited to create fragmentations, and the initial fragment mass values were generally lied in the brown dwarf mass regime.

Genevieve et al.[24] studied the dust clumps of the Protoplanetary Disk MWC 758 with the ALMA Band 6 observations from 2017 and 2021. They calibrated the raw visibility data with the Common Astronomy Software Application (CASA) versions, they put the inner disk as a reference and fitted a 2D Gaussian function to measure its centre. After they completed the self-calibration and data alignment, the continuum images were generated with the `tclean` function of CASA. They analyzed and reported the continuum images in 1.3 mm, and the proper motion of eccentric dust ring and dust clumps. They provided insights into the Keplerian and non-Keplerian alterations in the structure and dust clumps.

Sun

Kontar et al.[25] studied the type III solar radio burst accelerated electron behavior and developed a model and numerically tested it. They chose a nonlinear way to model this phenomenon with different relaxation for different locations and time. One of the paper’s main contributions is the explicit treatment of quasilinear theory and nonlinear diffusion. They provided the change in the peak electron number density in a nonlinear way with time or space and followed through the beam evolution.

Smith et al.[26] modelled the potential impacts of a nearby supernovae and interstellar cloud crossing on the solar system’s small bodies, Oort Cloud, and Kuiper Belt. They started with the remnant evidence of nearby supernovae in 3 and 7 million years ago from the ^{60}Fe , and examined the supernovae blast and cold cloud transit impacts on the solar system. They made these simulations on a Python environment with the `astropy`, `numpy`, `matplotlib`, and `scipy` packages. Among many interesting results, they reported that supernovae closer than 50 parsecs might have impacted Saturn’s Phoebe ring and swept away the Kuiper belt dust.

Mars

Pahlevan et al.[27] studied the origin of the Martian atmospheric volatiles. They considered the nebular capture through the Martian lifetime and outgassing primarily. They first discussed the literature and isotopic evidence on different types of contributions to the Martian atmosphere. From the different mixing and source contributions,

they considered a hybrid origin and also discussed the Martian hydrosphere origin and cometary contribution with isotopic ratios and the literature, too.

0.1 Jupiter

Arevalo et al.[28] constructed evolutionary models for Jupiter that accommodate not only the observed quantities by Voyager, Galileo, and Juno but also a fuzzy heavy-element core. They used their evolutionary code APPLE and important foci were the heavy element mass fractionations and the hydrogen/helium miscibility. Their models are compared to the equatorial radius of Jupiter. They considered irradiated atmospheric boundary conditions and utilized several works from the literature on the H-He equation of states (EOS), volume addition law, and multiphase EOS tables, including supercritical and superionic waters. They made several core evolution scenarios and reported that a fuzzy core for Jupiter was more likely.

0.2 Solar System Ice Giants

Ruiz et al.[29] simulated the dynamical evolution of Uranus and Neptune together with the modified REBOUND³ and Mercury v. 6.2 codes. They made several modifications to these codes without undermining how they would model the known initial conditions like Neptune and Uranus. These helped to explore larger parameter spaces. They reported that the new codes now can follow planetary evolution and explore their migration, orbital excitation, and damping.

Near-Earth Objects - Asteroids - Comets

Dobson et al.[30] analyzed the cometary activity of the newly-discovered Jupiter-family comet C/2023 RN₃ with 298 observations with the ATLAS, ZTF, LOOK, and Liverpool Telescope. They analyzed the evolution of its brightness, color, dust production rate (from the albedo, dust grain filling factor, and the aperture radius), and orbital evolution. They reported that the estimated cometary activity started on August 16, 2023, with no significant color change, a spatially-extended coma, a generally larger dust production rate considering Jupiter-family comets, and a semi-major axis change owing to an encounter with Jupiter.

³The relevant GitHub repository can be found here.

Moon

Brötzner et al.[31] measured laboratory *sputter*⁴ yields and compared them to the several modes of the SDTrimSP v 6.06 and SRIM 2013. They included both 1D and 3D simulations and as for the experiments, the material surface was examined with an atomic force microscopy. Rough surfaces also showed a lower amount of sputter, and simulations, especially for flat surfaces, overestimated the sputter in almost all incidence angles.

Giannakis et al.[32] studied ground penetrating radar data processing with deep learning methods. Using simulated data, they focused on the automatic full waveform inversion and missing/low quality trace filling. The related Kaggle Competition GDLC-1 is here.

Earth - Space relationship

Dalal et al.[33] studied the upstream ions towards the Earth and towards the Sun using *in situ* measurements from the L1 Lagrange point (H , 4He , and CNO species were analyzed). The data can be filtered and retrieved from here, which were collected by the Suprathermal Energetic Particle instrument T1 and T2 telescopes of the Wind spacecraft. They reported several interesting results, such as comparable softening in the upstream ion spectra with decreases in mass.

Zeebe and Kocken[34] reviewed the Astronomical (Milankovic) forcing of climate on tens of thousands of years timescale and the dating of geological timescales. They reviewed the concepts, and studies, and presented the available resources for different practical needs.

Magnetohydrodynamics

Sgynbayeva et al.[35] studied the circumplanetary disks, or the likelihood of them around different types of planets under different conditions, and also proposed ways for Jupiter and Saturn to have their current ring and satellite systems. They conducted their hydrodynamic simulations in Athena++. They simulated it for 100 planetary orbits for 0.3, 1, and 3 Jupiter-mass planets, and various other values for vertical height / radius, and thermal mass. They reported several cases where it is likely to have circumplanetary disks (CPD) and why we haven't yet observed much of them simultaneously, such as high-separation orbit amenable to having CPD but not so for direct imaging techniques.

⁴Solar wind hits the "airless" surface of celestial bodies, such as the moon, and ejects materials from that surface.

Last week in Analytical Chemistry

Author: *Yasin Güray Hatipoğlu*

The preprints summarized here were published between October 15 - October 21, 2024. They are more in nature of spectroscopy alone, and hence several studies regarding biochemistry, chromatography, and several other disciplines might be missed here.

Mass Spectroscopy

Ngan et al.[36] combined spectral matching in the non-target screening and machine learning techniques from Reverse-Phased Liquid Chromatography with High-Resolution Mass Spectrometry (RPLC-HRMS). Even though several studies tried to create databases of spectra and retention times, the variability in retention times according to the chromatographic conditions hindered the transferability of their data, the models they were based on, and so on. Hence, this study with three machine learning models and a focus on the retention index (RI)⁵, a more robust alternative to the retention time. The models are random forest regression with molecular fingerprints used to predict the RI, another random forest regression to predict RI from the MS/MS spectra, and a k-nearest neighbors binary classification to match ULSA annotation. They found the results promising and in forthe RI identification cases, successful.

Sehna et al.[37] from RECETOX⁶ constructed a pull-down-based⁷ pipeline EnDiTrap to detect endocrine-disrupting chemicals selectively and better. They also used this methodology for freshwater algal bloom sampling and retinoid-like active compound search. They used mass-spectrometry-based tandem quadrupole instruments in the target analysis, and also a nontarget high-resolution mass spectrometry (HRMS), and full scan MS^2 analysis. They applied orthogonal projections to the latent structures discriminant analysis (OPLS-DA) technique. While cautioning the implementers on different eluting solutions and other conditions on resulting measurements,

⁵Briefly, it is a kind of normalization that mitigates the instrumental-specific nature of retention times using two other n-alkane retention times that are eluted faster and slower than the analyte.

⁶Research Centre for Toxic Compounds in the Environment, Masaryk University.

⁷Pulling a sample and downing it to a specific protein to see how much of them bind that, briefly.

they found the undertaking successful and compared their post-Python processed results to the Compound Discoverer and MSDial.

Schmitt et al.[38] utilized LC-MS and an in-house spectral library for a more comprehensive metabolic profiling. They emphasized the pentafluorophenyl chromatography and extensive annotation positive impact on the predictive power, specifically for fasting blood glucose (very high R^2 , 0.97) and reasonably well for glomerular filtration rate⁸ calculated by elastic net-regularized linear and logistic regression. They used plasma samples from 432 patients.

Takemori et al.[39] introduced PEPPI-SP3 workflow (Passively Eluting Proteins from Polyacrylamide gels as Intact species for MS - single pot, solid-phase enhanced sample preparation) for an effective top-down proteomics⁹ approach. They used the mostly bottom-up analytics technique, SP3, after sodium dodecyl sulfate (SDS) polyacrylamide gel electrophoresis (PAGE) separation of proteins. They discussed the optimum choice for purifying the PEPPI remnants among the MCW (methanol-chloroform-water precipitation), FASP (filter aided sample preparation, in this case urea-assisted with ultrafiltration, and SP3, with several advantages for each of them while SP3 was generally more robust and overall superior.

Zhai et al.[40] coupled the size exclusion chromatography and native mass spectrometry (nano electron spray ionization (ESI) to mildly be able to increase the MS peak intensity with a more than one order of magnitude lower concentration solution in protein characterization. Moreover, they reported that the lower flow rate allowed them to bypass heated secondary gas use. They found the approach successful.

In order to provide a rapid and reliable method to diagnose lung cancer and similar biomolecule-containing aerosols, Chen et al.[41] presented the digitalMALDI. They tested it with insulin and the method was sensitive enough to detect as low as approx. 1 pg insulin in aerosol particles.

Immunoassays

Mao et al.[42] reviewed the digital immunoassay techniques and discussed their theoretical foundations, and made simulations and new techniques to further the absolute quantification of proteins through magnetic bead-related pro-

⁸There is more than one method to calculate glomerular filtration rate.

⁹Just like their names suggest, top-down approach utilizes the intact protein or its digestion products to characterize/identify the protein content, while bottom-up works from much smaller peptides to uncover the undigested unique chains.

cesses and compared their methods to the single molecule immunoassay and electrochemiluminescence immunoassay. The related GitHub repository for these studies are here.

Electrochemistry

D'Antona et al.[43] examined the proton transfer through the interface between two immiscible electrolyte solutions (ITIES) to uncover the ion transfer kinetics at such regions. They experimented with different solutions and exchange current densities, and interpreted both experimental and COMSOL multiphysics simulation results together. The chemical 2,6-diphenylpyridine (DPP) favored the direct proton transfer across the hydrochloric acid (HCl_{aq} —Trifluorotoluene interface according to the cyclic voltammetry and aforementioned experimental/simulation results.

Nuclear Magnetic Resonance - NMR

Pais, Reile, and Ausmees[44] mitigated the problem of too-low concentration in the conventional nuclear magnetic resonance (NMR) analyses by using non-hydrogenative parahydrogen induced polarization (nh-PHIP). This technique results in analyte-related peaks in a conventional-NMR blank regions with the transient iridium complex coordinate compounds through the interactions with the parahydrogens in the complex. They found their complex successful in blood sample adenine phosphonucleotide analyses. The resulting shape of the octahedral Iridium complex had two 1-methyl-1,2,3-triazol substrates and (IMes) = 1,3-bis(2,4,6-trimethylphenyl)imidazol-2-ylidene.

Fluorescence

Roy et al.[45] studied a specific method to detect inorganic polyphosphate while not getting interference from cyclic metaphosphates and biological polyphosphates, pyrophosphate, and ATP, ADP, and GTP. The name of their technique is the excited state intramolecular proton transfer-based (ESIPT) fluorescent turn-on sensors. The sensor chemicals complexation with copper cations results in fluorescent quenching at will. Their sensor chemical was 2-hydroxy-phenyl-benzoxazole derivatives, where their nitrogen and hydroxyl-oxygen played the complexing agent role. They were successful in making a reversible, selective sensor and even were able to monitor polyphosphate digestion using these sensors.

Last week in Remote Sensing

Author: Yasin Güray Hatipoğlu

The preprints summarized here were published between October 15 - October 21, 2024. These are generally based on the preprints retrieved when “remote sensing” words are given between quotation marks within arXiv’s cs.CV and similar cross-fields.

Tao et al.[46] reviewed the recent advancements in the visual language models for remote sensing tasks, where the enhancements took place, and provided future directions.

Segmentation

Mahara et al.[47] introduced the Dense Depth-wise Dilated Separable Spatial Pyramid Pooling (DenseDDSSPP) with the DeepLabV3+ for road extraction from remote sensing images. The data they used were the Massachusetts Road Dataset and DeepGlobe Road Dataset. They reported the optimal backbone network as Xception among others, such as VGG19, ResNet50, and more. Their proposed model outperformed U-Net, DeepLabV3+ with ASSP instead of DenseDDSSPP, SegNet, D-LinkNet, and Attention-UNet in both datasets and was the second best in terms of F1 score after RFE-LinkNet, while it was the best in IoU and Precision metrics.

Liu et al.[48] developed the Adaptive Disaster Interpretation (ADI) that goes beyond an individual segmentation or object detection approach by combining such tasks with also large language models using autonomous agents. They provided the RescueADI dataset to develop and test their novel method. They improved upon Visual Question Answering (like the number of vehicles on a scene) to the planning and reporting in the ADI. The basic categories of annotated requests that ADI can work with are 1) Rescue Path Search, 2) Object Perception, 3) Basic Task Execution (like locating buildings), and 4) Fine-grained damage assessment. Their method outperformed the GeoChat and visualGLM in all tasks checked, and among the chosen LLM backends, GPT 4o mini generally outperformed Deepseek 7b, Qwen1.5 7b, Qwen2.5 7b, and Llama3.1 8b.

Ma et al.[49] finetuned MANet segment anything model for the multimodal remote sensing scene semantic segmentation task. The relevant code was said to be available in the following GitHub repository. They introduced a novel adapter, MMAadapter which extracted and fused multimodal remote sensing features to finetune a

segment anything module and worked with the ISPRS Vaihingen and ISPRS Potsdam datasets to compare MANet’s performance, and it was the best-performing algorithm in most classes and metrics.

Modelling-Forecast

Hirner and Fraundorfer[50] developed SAda-Net¹⁰ to make a self-supervised stereo estimation from unannotated data with convolutional neural network approach having 495 thousands of trainable weights, comparatively lightweight. In the end, they took stereo-rectified satellite image tiles and generated a point cloud and digital surface models after the feature extraction, similarity function, and disparity maps. They trained the model with the SpaceNet challenge dataset of WorldView-3 panchromatic satellite images. They also showcase the superiority of their method using the Jacksonville data, Middlebury, and KITTI2015.

Object Detection

Ren et al.[51] introduced the RemoteDet-Mamba, the hybrid Mamba-CNN network with a cross-modal fusion Mamba module for the object detection tasks from remote sensing images. they focused on UAV data as inputs. The dataset was the DroneVehicle, 28439 visible and infrared image pairs with a total of 953087 detection instances. They evaluated the performance with the mean average precision metric. For comparison, the chosen rival methodologies were as follows: RetianNet, Refined rotation RetianNet, Single-shot alignment networks, Faster R-CNN, Region of Interest Transformer, Rotation equivariant detector, uncertainty-aware cross-modality vehicle detection, Multimodal Knowledge Distillation, Two-stream Feature Alignment Detector, Calibrated and complementary Transformer, and Disparity-guided multispectral Mamba. Their method performed better than others in terms of car, truck, freight car, bus, and van detections, mAP metric, and model size, and it was moderately fast between the slower and faster choices.

¹⁰The algorithm and details can be found in the following GitHub repository.

Last week in Environmental Chemistry

Author: Yasin Güray Hatipoğlu

The preprints summarized here were published between October 15 - October 21, 2024 in chemRxiv's Earth, Space, and Environmental chemistry preprints are being surveyed, and unfortunately, not many preprints are published under environmental topics in this field.

Li et al.[52] utilized liquid chromatography-high resolution mass spectrometry (LC-HRMS) with iodine kinetics to identify different classes of organic peroxides in α -pinene¹¹ secondary organic aerosols (SOA). They first checked the iodine-related kinetics of commercially available organic peroxides, then analyzed the SOA they generated with the iodometry-assisted LC-HRMS and non-target analysis. They stated that the added specificity gained from the iodometry can aid in organic peroxide identification for atmospheric studies as well.

Murphy[53] presented a novel fluorescence index ARIX to determine the dissolved organic compound structure and aromaticity. There are already several indices, such as the fluorescence index, biological index, humification index, or PARIX from a study using the PARAFAC analysis components (one peaked around 500 nm and another around 400 nm) ratio to each other. This study reanalyzed the available data (9 datasets with more than a thousand data points) to circumvent factor analysis-related potentially dataset-specific factors and develop a more generalizable model, ARIX. The focus was on predicting the specific UV absorbance (SUVA) by these indices, and the relations between the predictions and actual measurements were satisfactory.

Petric et al.[54] comprehensively reviewed the meteorological normalization/deweathering step in air pollutant concentration prediction workflows from the literature and presented the assumptions, pitfalls, and limitations. They clarified two propositions regarding them and conducted three numerical experiments in Python numpy, and scikit-learn packages on the normalization in 1) correlated inputs, 2) forecasting, and 3) extrapolating cases. They provided several alternative ways to mitigate the present problems in resampling and normalization cases.

¹¹They expose this chemical to ozone and generate organic aerosols as a result of that.

Last week in Data Decomposition/Transformation

Author: Yasin Güray Hatipoğlu

The preprints summarized here were published between October 15 - October 21, 2024. This is generally from arXiv's stat.ML or stat.ME cross-list. The section focuses on preprints heavily worked with or developed data decomposition/transformation techniques, such as principal component analysis (PCA) or Fourier Transformation.

Denoising

Cao et al.[55] made a network-related denoising algorithm, a variant of the lifting one coefficient at a time (LOCAAT) line graph (LG-LOCAAT) using the data from the Hydrology Data Explorer of the United Kingdom. As a river is much more than just the sampling points, it is intuitive to think that a better consideration of the entire river network in the denoising step produces more accurate results. The river network water flow/quality data has always errors to varying extent and it is nontrivial to model these inhomogeneously-sampled points with a graph network or similar approaches. The main concepts behind this approach are line graph conceptualization of the river network and wavelet decomposition methods. They made both simulation analyses and worked with the real river water quality data (dissolved oxygen). The information for the new vertices was estimated via Euclidean distances between the vertices. The algorithm has the Split, Predict, Update, and Relink steps and the iterations of that order for weight updates. The algorithm performed well for both the simulation and real-world cases.

Modelling

Sinha et al.[56] utilized a *disentanglement* routine for the explainable deep learning model creation. Similar to exploratory factor analysis, the inferences from the data were attempted to be examined under the latent generative factors for a more explainable model overall. This has been done by a structural causal model in this paper, and a variational autoencoder tried to learn them. Their datasets were D-Sprites with 6 independent generative factors consisting of 737280 images, and Shapes3D with again 6 independent factors with 480000 images. They found their method successful in identifying causal factors.

Tang et al.[57] examined the canonical polyadic tensor decomposition concept with unaligned observations. They applied their new methodology to the synthetic data for numerical tests and also to the early childhood human microbiome dataset. The loss mechanisms tested were l2-loss and general loss (and among the examples, Poisson loss). They implemented a sketching algorithm for higher efficiency while using l2-loss, and an optimization algorithm besides stochastic gradient.

Li et al.[58] worked on root cause identification and utilized permutations and the Cholesky decomposition (decomposing a matrix A to LL^*) for this purpose in the rare genetic disease source gene search. They started with a directed acyclic graph to show the causality and identified 3 out of 5 options with three descendants as the intervention root cause. They discussed that if the root cause is identifiable at all, then tried to reduce the required/sufficient number of permutations to identify the root cause, apply this method to the high-dimensional settings and a disease-causing gene expression dataset¹² later on. The high-dimensional scenario utilized a cross-validated Lasso in a node-by-node way and interpreted the results according to the expected scenarios whether or not a specific node is a root cause. They found the new approach promising.

Missing Data Imputation

Feitelberg et al.[59] studied the matrix completion problem over distribution functions and how they can successfully complete missing data with a proper latent factor model considering the Wasserstein norm. They start with a simulated dataset with missing/unobserved entries: Three schools, three different courses with and without digital resources (6 dimensions), and 100 data-points in each except four of them devoid of entries. They had a Lipschitz latent factor model on Wasserstein space. Their completion approach was nearest-neighbor-like, rather than singular value-based ones. They showed that their method improved the estimation compared to only using the observed values.

¹²Here are the Zenodo links for the strand-specific and non-strand-specific datasets.

References

- [1] Armen Tokadjian, Renyu Hu, and Mario Damiano. The detectability of $\text{ch}_4/\text{co}_2/\text{co}$ and n_2o biosignatures through reflection spectroscopy of terrestrial exoplanets. *arXiv*, 2024. URL <https://arxiv.org/abs/2410.14848v1>.
- [2] Natsuko Yamaguchi and Kareem El-Badry. A search for self-lensing binaries with tess and constraints on their occurrence rate. *arXiv*, 2024. URL <https://arxiv.org/abs/2410.13939v1>.
- [3] Christopher E. O’Connor and Dong Lai. Metal pollution in sun-like stars from destruction of ultra-short-period planets. *arXiv*, 2024. URL <https://arxiv.org/abs/2410.11935v1>.
- [4] Aviv Ofir, Gideon Yoffe, and Oded Aharonson. Planetary mass determinations from a simplified photodynamical model – application to the complete kepler dataset. *arXiv*, 2024. URL <https://arxiv.org/abs/2410.11401v1>.
- [5] Zifan Lin, Saverio Cambioni, and Sara Seager. Most high-density exoplanets are unlikely to be remnant giant-planet cores. *arXiv*, 2024. URL <https://arxiv.org/abs/2410.12640v1>.
- [6] Clément Staelen, Jean-Marc Huré, Anaïs Meunier, and Pauline Noé. Existence of slowly rotating bipolytropes with prolate cores. *arXiv*, 2024. URL <https://arxiv.org/abs/2410.14482v1>.
- [7] Giuseppe Pucacco. Dynamical stability of the laplace resonance. *arXiv*, 2024. URL <https://arxiv.org/abs/2410.12768v1>.
- [8] Haochuan Yu, Suzanne Aigrain, Baptiste Klein, Michael Cretignier, Florian Lienhard, and Stephen J. Roberts. A gaussian process model for stellar activity in 2-d line profile time-series. *arXiv*, 2024. URL <https://arxiv.org/abs/2410.12698v1>.
- [9] Song Wang, Xue Li, Hengheng Han, and Jifeng Liu. Predicting photospheric uv emission from stellar evolutionary models. *arXiv*, 2024. URL <https://arxiv.org/abs/2410.11611v1>.
- [10] Alexander Venner, Qier An, Chelsea X. Huang, Timothy D. Brandt, Robert A. Wittenmyer, and Andrew Vanderburg. Hd 28185 revisited: An outer planet, instead of a brown dwarf, on a saturn-like orbit. *arXiv*, 2024. URL <https://arxiv.org/abs/2410.14218v1>.
- [11] Samuel Whitebook, Timothy Brandt, Gregory Mirek Brandt, and Emily Martin. Discovery of the binarity of gliese 229b, and constraints on the system’s properties. *arXiv*, 2024. URL <https://arxiv.org/abs/2410.11999v1>.
- [12] Jerry W. Xuan, A. Mérand, W. Thompson, Y. Zhang, S. Lacour, D. Blakely, D. Mawet, R. Oppenheimer, J. Kammerer, K. Batygin, A. Sanghi, J. Wang, J. B. Ruffio, M. C. Liu, H. Knutson, W. Brandner, A. Burgasser, E. Rickman, R. Bowens-Rubin, M. Salama, W. Balmer, S. Blunt, G. Bourdarot, P. Caselli, G. Chauvin, R. Davies, A. Drescher, A. Eckart, F. Eisenhauer, M. Fabricius, H. Feuchtgruber, G. Finger, N. M. Förster Schreiber, P. Garcia, R. Genzel, S. Gillessen, S. Grant, M. Hartl, F. Haußmann, T. Henning, S. Hinkley, S. F. Höning, M. Horrobin, M. Houllé, M. Janson, P. Kervella, Q. Kral, L. Kreidberg, J. B. Le Bouquin, D. Lutz, F. Mang, G. D. Marleau, F. Millour, N. More, M. Nowak, T. Ott, G. Otten, T. Paumard, S. Rabien, C. Rau, D. C. Ribeiro, M. Sadun Bordoni, J. Sauter, J. Shangquan, T. T. Shimizu, C. Sykes, A. Soulain, S. Spezzano, C. Straubmeier, T. Stolker, E. Sturm, M. Subroweit, L. J. Tacconi, E. F. van Dishoeck, A. Vigan, F. Widmann, E. Wieprecht, T. O. Winterhalder, and J. Woillez. The cool brown dwarf gliese 229 b is a close binary. *arXiv*, 2024. URL <https://arxiv.org/abs/2410.11953v1>.
- [13] Yui Kawashima, Hajime Kawahara, Yui Kasagi, Hiroyuki Tako Ishikawa, Kento Masuda, Takayuki Kotani, Tamoyuki Kudo, Teruyuki Hirano, Masayuki Kuzuhara, Stevanus K Nugroho, John Livingston, Hiroki Harakawa, Jun Nishikawa, Masashi Omiya, Takuya Takarada, Motohide Tamura, and Akitoshi Ueda. Atmospheric retrieval of subaru/ird high-resolution spectrum of the archetype t-type brown dwarf gl 229 b. *arXiv*, 2024. URL <https://arxiv.org/abs/2410.11561v1>.
- [14] Kevin Marimbu and Eve J. Lee. On the dynamical erasure of initial conditions in multi-planetary systems. *arXiv*, 2024. URL <https://arxiv.org/abs/2410.14782v1>.
- [15] Arnav Agrawal and Ryan J. MacDonald. Cthulhu: An open source molecular and atomic cross section computation code for

- substellar atmospheres. *arXiv*, 2024. URL <https://arxiv.org/abs/2410.14751v1>.
- [16] Vikas Soni and Kinsuk Acharyya. Signature of vertical mixing in hydrogen-dominated exoplanet atmospheres. *arXiv*, 2024. URL <https://arxiv.org/abs/2410.12737v1>.
- [17] M. Stangret, L. Fossati, M. C. D’Arpa, F. Borsa, V. Nascimbeni, L. Malavolta, D. Sicilia, L. Pino, F. Biassoni, A. S. Bonomo, M. Brogi, R. Claudi, M. Damasso, C. Di Maio, P. Giacobbe, G. Guilluy, A. Harutyunyan, A. F. Lanza, A. F. Martinez Fiorenzano, L. Mancini, D. Nardiello, G. Scandariato, A. Sozzetti, and T. Zingales. The gaps programme at tng: Tbd. studies of atmospheric feii winds in ultra-hot jupiters kelt-9b and kelt-20b using harps-n spectrograph. *arXiv*, 2024. URL <https://arxiv.org/abs/2410.11731v1>.
- [18] Lorenzo Cesario, Tim Lichtenberg, Eleonora Alei, Óscar Carrión-González, Felix A. Dannert, Denis Defrère, Steve Ertel, Andrea Fortier, A. García Muñoz, Adrian M. Glauser, Jonah T. Hansen, Ravit Helled, Philipp A. Huber, Michael J. Ireland, Jens Kammerer, Romain Laugier, Jorge Lillo-Box, Franziska Menti, Michael R. Meyer, Lena Noack, Sascha P. Quanz, Andreas Quirrenbach, Sarah Rugheimer, Floris van der Tak, Haiyang S. Wang, Marius Anger, Olga Balsalobre-Ruza, Surendra Bhattarai, Marrick Braam, Amadeo Castro-González, Charles S. Cockell, Tereza Constantinou, Charles S. Cockell, Tereza Constantinou, Gabriele Cugno, Jeanne Davoult, Manuel Güdel, Nina Hernitschek, Sasha Hinkley, Satoshi Itoh, Markus Janson, Anders Johansen, Hugh R. A. Jones, Stephen R. Kane, Tim A. van Kempen, Kristina G. Kislyakova, Judith Korth, Andjelka B. Kovacevic, Stefan Kraus, Rolf Kuiper, Joice Mathew, Taro Matsuo, Yamila Miguel, Michiel Min, Ramon Navarro, Ramses M. Ramirez, Heike Rauer, Berke Vow Ricketti, Amedeo Romagnolo, Martin Schlecker, Evan L. Sneed, Vito Squicciarini, Keivan G. Stassun, Motohide Tamura, Daniel Viudez-Moreiras, Robin D. Wordsworth, and the LIFE Collaboration. Large interferometer for exoplanets (life). xiv. finding terrestrial protoplanets in the galactic neighborhood. *arXiv*, 2024. URL <https://arxiv.org/abs/2410.13457v1>.
- [19] Erica Dykes, Thayne Currie, Kellen Lawson, Miles Lucas, Tomoyuki Kudo, Minghan Chen, Olivier Guyon, Tyler D Groff, Julien Lozi, Jeffrey Chilcote, Timothy D. Brandt, Sebastien Vievard, Nour Skaf, Vincent Deo, Mona El Morsy, Danielle Bovie, Taichi Uyama, Carol Grady, Michael Sitko, Jun Hashimoto, Frantz Martinache, Nemanja Jovanovic, Motohide Tamura, and N. Jeremy Kasdin. Scexao/charis near-infrared scattered-light imaging and integral field spectropolarimetry of the ab aurigae protoplanetary system. *arXiv*, 2024. URL <https://arxiv.org/abs/2410.11939v1>.
- [20] Viktória Fröhlich and Zsolt Regály. Origin of ca ii emission around polluted white dwarfs. *arXiv*, 2024. URL <https://arxiv.org/abs/2410.15084v1>.
- [21] A. Zuleta, T. Birnstiel, and R. Teague. Kinematical signatures: Distinguishing between warps and radial flows. *arXiv*, 2024. URL <https://arxiv.org/abs/2410.14457v1>.
- [22] Alexandros Ziampras, Cornelis P. Dullemond, Tilman Birnstiel, Myriam Benisty, and Richard P. Nelson. Spirals, rings, and vortices shaped by shadows in protoplanetary disks: from radiative hydrodynamical simulations to observable signatures. *arXiv*, 2024. URL <https://arxiv.org/abs/2410.13932v1>.
- [23] Wenrui Xu, Yan-Fei Jiang, Matthew W. Kunz, and James M. Stone. Global simulations of gravitational instability in protostellar disks with full radiation transport. i. stochastic fragmentation with optical-depth-dependent rate and universal fragment mass. *arXiv*, 2024. URL <https://arxiv.org/abs/2410.12042v1>.
- [24] I-Hsuan Genevieve Kuo, Hsi-Wei Yen, and Pin-Gao Gu. Alma observations of proper motions of the dust clumps in the protoplanetary disk mwc 758. *arXiv*, 2024. URL <https://arxiv.org/abs/2410.11679v1>.
- [25] Eduard P. Kontar, Francesco Azzollini, and Olena Lyubchik. Advection-nonlinear-diffusion model of flare accelerated electron transport in type iii solar radio bursts. *arXiv*, 2024. URL <https://arxiv.org/abs/2410.11409v1>.
- [26] Leeanne Smith, Jesse A. Miller, and Brian D. Fields. Nearby supernova and cloud crossing effects on the orbits of small bodies in the solar system. *arXiv*, 2024. URL <https://arxiv.org/abs/2410.12275v1>.
- [27] Kaveh Pahlevan, Laura Schaefer, and Don Porcelli. A hybrid origin for the martian atmosphere. *arXiv*, 2024. URL <https://arxiv.org/abs/2410.15508v1>.

- [28] Roberto Tejada Arevalo, Ankan Sur, Yubo Su, and Adam Burrows. Jupiter evolutionary models incorporating stably stratified regions. *arXiv*, 2024. URL <https://arxiv.org/abs/2410.12899v1>.
- [29] Arcelia Hermosillo Ruiz, Ruth Murray-Clay, Kathryn Volk, and Rosemary Pike. Forcing planets to evolve: The relationship between uranus and neptune at late stages of dynamical evolution. *arXiv*, 2024. URL <https://arxiv.org/abs/2410.11813v1>.
- [30] Matthew M. Dobson, Megan E. Schwamb, Alan Fitzsimmons, Michael S. P. Kelley, Carrie E. Holt, Joseph Murtagh, Henry H. Hsieh, Larry Denneau, Nicolas Erasmus, A. N. Heinze, Luke J. Shingles, Robert J. Siverd, Ken W. Smith, John L. Tonry, Henry Weiland, David. R. Young, Tim Lister, Edward Gomez, Joey Chatelain, and Sarah Greenstreet. Analysing the onset of cometary activity by the jupiter-family comet 2023 rn3. *arXiv*, 2024. URL <https://arxiv.org/abs/2410.13644v1>.
- [31] Johannes Brötzner, Herbert Biber, Paul Stefan Szabo, Noah Jäggi, Lea Fuchs, Andreas Nanning, Martina Fellingner, Gyula Nagy, Eduardo Pitthan, Daniel Primetzhofer, Andreas Mutzke, Richard Arthur Wilhelm, Peter Wurz, André Galli, and Friedrich Aumayr. Sputter yields of the lunar surface: Experimental validation and numerical modelling of solar wind sputtering of apollo 16 soils. *arXiv*, 2024. URL <https://arxiv.org/abs/2410.14450v1>.
- [32] Iraklis Giannakis, Craig Warren, Antonios Giannopoulos, Georgios Leontidis, Yan Su, Feng Zhou, Javier Martin-Torres, and Nectaria Diamanti. Investigating the capabilities of deep learning for processing and interpreting one-shot multi-offset gpr data: A numerical case study for lunar and martian environments. *arXiv*, 2024. URL <https://arxiv.org/abs/2410.14386v1>.
- [33] Bijoy Dalal, Dibyendu Chakrabarty, Christina M. S. Cohen, and Nandita Srivastava. Investigation on upstream ion events from 11 point observation: New insights. *arXiv*, 2024. URL <https://arxiv.org/abs/2410.13243v1>.
- [34] Richard E. Zeebe and Ilja J. Kocken. Applying astronomical solutions and milanković forcing in the earth sciences. *arXiv*, 2024. URL <https://arxiv.org/abs/2410.12977v1>.
- [35] Sabina Sagynbayeva, Rixin Li, Aleksandra Kuznetsova, Zhaohuan Zhu, Yan-Fei Jiang, and Philip J. Armitage. Circumplanetary disks are rare around planets at large orbital radii: A parameter survey of flow morphology around giant planets. *arXiv*, 2024. URL <https://arxiv.org/abs/2410.14896v1>.
- [36] Hiu Lok Ngan, Viktoriia Turkina, Denice van Herwerden, Hong Yan, Zongwei Cai, and Saer Samanipour. Integration of transferable prediction of retention index and universal library search enhances exposome identification probability in rplc/hrms-based non-targeted analysis. 2024. URL <https://chemrxiv.org/engage/chemrxiv/article-details/670a43adcec5d6c142ed957a>.
- [37] Ludek Sehnal, Garry Codling, Marie Smutná, Roman Grabic, and Klára Hilscherová. Enditrap: Pull-down-based pipeline for detection of endocrine-disrupting chemicals. 2024. URL <https://chemrxiv.org/engage/chemrxiv/article-details/670d0ac312ff75c3a1621aad>.
- [38] Fabian Constantin Schmitt, Vincent ten Cate, Zlatka Fischer, Mathias Hagen, Barbara A Steigenberger, Stefan Tenzer, Philipp S Wild, and Thierry Schmidlin. Metabolic profiling of the emdia cohort by a scalable dia-lc-ms workflow. 2024. URL <https://chemrxiv.org/engage/chemrxiv/article-details/670e647acec5d6c142390042>.
- [39] Ayako Takemori, Naoyuki Sugiyama, Jake Kline, Luca Fornelli, and Nobuaki Takemori. Gel-based sample fractionation with sp3-purification for top-down proteomics. 2024. URL <https://chemrxiv.org/engage/chemrxiv/article-details/670fa4ab12ff75c3a199058f>.
- [40] Ziran Zhai and Andrea FG Gargano. Nanoflow size exclusion chromatography-native mass spectrometry of intact proteoforms and protein complexes. 2024. URL <https://chemrxiv.org/engage/chemrxiv/article-details/6710c9e5cec5d6c142669e5b>.
- [41] Dapeng Chen, Wayne Bryden, Michael McLoughlin, Scott Ecelberger, Timothy Cornish, and Lara Moore. digitalmaldi: A single particle-based mass spectrometric detection system for biomolecules. 2024. URL <https://chemrxiv.org/engage/chemrxiv/article-details/67114655cec5d6c142706eef>.

- [42] Tianjiao Mao, Liang Lu, Yipi Xiao, Fanrong Ai, Liang Guo, Jiani Wang, Jing Yao, Xiluan Yan, and Huan Li. Development of absolute quantification methods for digital immunoassays: Theoretical framework and establishment of droplet-based digital immunoassay techniques. 2024. URL <https://chemrxiv.org/engage/chemrxiv/article-details/66f0cab851558a15efd10dc2>.
- [43] Nick D’Antona, Nadia Barnard, Shane Ardo, Yixian Wang, Yogesh Surendranath, Paul Kempler, and Shannon Boettcher. Proton-transfer kinetics at liquid-liquid interfaces. 2024. URL <https://chemrxiv.org/engage/chemrxiv/article-details/6711347c51558a15ef5b05e6>.
- [44] Helen Pais, Indrek Reile, and Kerti Ausmees. Analysis of adenosine phosphonucleotides in blood by nh-pph. 2024. URL <https://chemrxiv.org/engage/chemrxiv/article-details/670d8e3051558a15ef130631>.
- [45] Subhra Roy, Sandra Moser, Tobias Dürr-Mayer, Rahel Hinkelmann, and Henning Jessen. Esipt fluorescence turn-on sensors for detection of short chain inorganic polyphosphate in water. 2024. URL <https://chemrxiv.org/engage/chemrxiv/article-details/670819a112ff75c3a1130890>.
- [46] Lijie Tao, Haokui Zhang, Haizhao Jing, Yu Liu, Kelu Yao, Chao Li, and Xizhe Xue. Advancements in visual language models for remote sensing: Datasets, capabilities, and enhancement techniques. *arXiv*, 2024. URL <https://arxiv.org/abs/2410.17283v1>.
- [47] Arpan Mahara, Md Rezaul Karim Khan, Naphtali D. Rishe, Wenjia Wang, and Seyed Masoud Sadjadi. Automated road extraction from satellite imagery integrating dense depthwise dilated separable spatial pyramid pooling with deeplabv3+. *arXiv*, 2024. URL <https://arxiv.org/abs/2410.14836v1>.
- [48] Zhuoran Liu, Danpei Zhao, and Bo Yuan. Rescueadi: Adaptive disaster interpretation in remote sensing images with autonomous agents. *arXiv*, 2024. URL <https://arxiv.org/abs/2410.13384v1>.
- [49] Xianping Ma, Xiaokang Zhang, Man-On Pun, and Bo Huang. Manet: Fine-tuning segment anything model for multimodal remote sensing semantic segmentation. *arXiv*, 2024. URL <https://arxiv.org/abs/2410.11160v1>.
- [50] Dominik Hirner and Friedrich Fraundorfer. Sada-net: A self-supervised adaptive stereo estimation cnn for remote sensing image data. *arXiv*, 2024. URL <https://arxiv.org/abs/2410.13500v1>.
- [51] Kejun Ren, Xin Wu, Lianming Xu, and Li Wang. Remotedet-mamba: A hybrid mamba-cnn network for multi-modal object detection in remote sensing images. *arXiv*, 2024. URL <https://arxiv.org/abs/2410.13532v1>.
- [52] Kangwei Li, Zhensen Zheng, Julian Resch, Jialiang Ma, and Markus Kalberer. Molecular composition of organic peroxides in secondary organic aerosols revealed by peroxide-iodide reactivity. 2024. URL <https://chemrxiv.org/engage/chemrxiv/article-details/671020f8cec5d6c1425c3f31>.
- [53] Kathleen Murphy. A global fluorescence index for predicting dissolved organic carbon abundance and aromaticity. 2024. URL <https://chemrxiv.org/engage/chemrxiv/article-details/6703ed1712ff75c3a1b74141>.
- [54] Valentino Petrić, Mario Lovrić, and Bernhard C Geiger. Meteorological normalization or deweathering for predicting air pollutant concentration: Pitfalls and limitations. 2024. URL <https://chemrxiv.org/engage/chemrxiv/article-details/67126f38cec5d6c14285002e>.
- [55] Dingjia Cao, Marina I. Knight, and Guy P. Nason. A multiscale method for data collected from network edges via the line graph. *arXiv*, 2024. URL <https://arxiv.org/abs/2410.13693v1>.
- [56] Sanchit Sinha, Guangzhi Xiong, and Aidong Zhang. Structural causality-based generalizable concept discovery models. *arXiv*, 2024. URL <https://arxiv.org/abs/2410.15491v1>.
- [57] Runshi Tang, Tamara Kolda, and Anru R. Zhang. Tensor decomposition with unaligned observations. *arXiv*, 2024. URL <https://arxiv.org/abs/2410.14046v1>.
- [58] Jinzhou Li, Benjamin B. Chu, Ines F. Scheller, Julien Gagneur, and Marloes H. Maathuis. Root cause discovery via permutations and cholesky decomposition. *arXiv*,

2024. URL <https://arxiv.org/abs/2410.12151v1>.

- [59] Jacob Feitelberg, Kyuseong Choi, Anish Agarwal, and Raaz Dwivedi. Distributional matrix completion via nearest neighbors in the wasserstein space. *arXiv*, 2024. URL <https://arxiv.org/abs/2410.13112v1>.